Powering DNA Repair through Substrate Electrostatic Interactions†

Yu Lin Jiang,‡ Yoshitaka Ichikawa,§ Fenhong Song,|| and James T. Stivers*,‡

Department of Pharmacology and Molecular Sciences, The Johns Hopkins University School of Medicine, 725 North Wolfe Street, Baltimore, Maryland 21205-2185, Optimer Pharmaceuticals, Inc., 10130 Sorrento Valley Road, Suite D, San Diego, California 92121, and Center for Advanced Research in Biotechnology, National Institute of Standards and Technology and University of Maryland Biotechnology Institute, Rockville, Maryland 20850

Received October 16, 2002; Revised Manuscript Received December 18, 2002

ABSTRACT: The reaction catalyzed by the DNA repair enzyme uracil DNA glycosylase (UDG) proceeds through an unprecedented stepwise mechanism involving a positively charged oxacarbenium ion sugar and uracil anion leaving group. Here we use a novel approach to evaluate the catalytic contribution of electrostatic interactions between four essential phosphodiester groups of the DNA substrate and the cationic transition state. Our strategy was to substitute each of these phosphate groups with an uncharged (*R*)- or (*S*)-methylphosphonate linkage (MeP). We then compared the damaging effects of these methylphosphonate substitutions on catalysis with their damaging effects on binding of a cationic 1-azadeoxyribose (1-aza-dR$^+$) oxacarbenium ion analogue to the UDG−uracil anion binary complex. A plot of log k_{cat}/K_m for the series of MeP-substituted substrates against log K_D for binding of the 1-aza-dR$^+$ inhibitors gives a linear correlation of unit slope, confirming that the electronic features of the transition state resemble that of the 1-aza-dR$^+$, and that the anionic backbone of DNA is used in transition state stabilization. We estimate that all of the combined phosphodiester interactions with the substrate contribute 6−8 kcal/mol toward lowering the activation barrier, a stabilization that is significant compared to the 16 kcal/mol catalytic power of UDG. However, unlike groups of the enzyme that selectively stabilize the charged transition state by an estimated 7 kcal/mol, these phosphodiester groups also interact strongly in the ground state. To our knowledge, these results provide the first experimental evidence for electrostatic stabilization of a charged enzymatic transition state and intermediate using the anionic backbone of DNA.

The appearance of uracil in DNA through the deamination of cytosine or misincorporation of dUMP during DNA synthesis produces a relentless source of DNA damage that must be reversed through the action of the uracil base excision repair pathway (*3*). The first enzyme in this pathway is uracil DNA glycosylase (UDG), the powerful enzyme that hydrolyzes the glycosidic bond of deoxyuridine (dU) in DNA, lowering the activation barrier by 16 kcal/mol as compared to the spontaneous reaction at 25 °C (*4*).

In recent years, mechanistic and structural studies of the UDG-catalyzed reaction have reached the highest levels of detail (*5*, *6*), allowing the first snapshot of a DNA repair glycosylase transition state using kinetic isotope effect methods (*7*). These studies established a remarkable stepwise mechanism for cleavage of the glycosidic bond of dU involving a positively charged oxacarbenium ion sugar and a negatively charged uracil leaving group (Figure 1). Subsequent mutagenesis and inhibition studies using 1-aza-deoxyribose (1-aza-dR$^+$) oxacarbenium ion analogues have provided further support for this novel ionic intermediate (*8*, *9*). An "electrostatic sandwich" mechanism was strongly suggested in which the cationic sugar was stabilized by an anionic aspartate located beneath the sugar ring, and the uracil anion leaving group above the ring (Figure 1). The catalytic benefit from these interactions (7 kcal/mol) is a significant part of the catalytic power of UDG, and likely

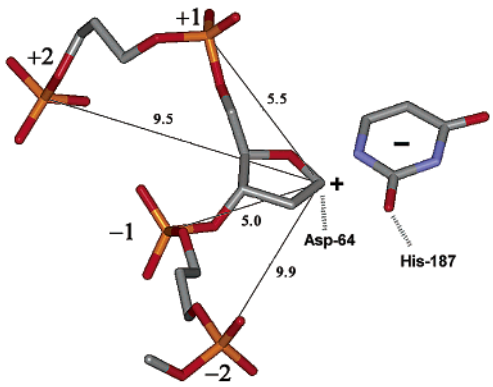

FIGURE 1: Oxacarbenium ion−uracil anion intermediate of the UDG-catalyzed reaction showing the distances (angstroms) between the four important phosphodiester groups of the substrate and the anomeric carbon. The model is derived from the crystal structure of UDG bound to deoxypseudouridine-containing substrate analogue DNA and from KIE measurements by removing the glycosidic bond (*5*, *20*). The numbering system for the phosphodiester groups is indicated. The two enzyme groups (Asp64 and His187) involved in the electrostatic sandwich mechanism for oxacarbenium ion stabilization are also indicated (see the text).

† This work was supported by National Institutes of Health Grant GM56834 (J.T.S.).

* To whom correspondence should be addressed. Telephone: (410) 502-2758. Fax: (410) 955-3023. E-mail: jstivers@jhmi.edu.

‡ The Johns Hopkins University School of Medicine.

§ Optimer Pharmaceuticals, Inc.

|| National Institute of Standards and Technology and University of Maryland Biotechnology Institute.

10.1021/bi027014x CCC: $25.00
Published on Web 01/30/2003

plays a role in promoting the remarkable stepwise mechanism (*9*).

A stepwise mechanism has also been proposed on the basis of QM/MM simulations of the enzymatic reaction surface (*10*). A provocative suggestion derived from the computational work was that electrostatic interactions derived from four negatively charged phosphodiester groups of the substrate were used to stabilize the cationic sugar in the transition state and intermediate by 17.5−21.9 kcal/mol, suggesting that "substrate autocatalysis" provided essentially the entire energetic basis for UDG catalysis (Figure 1). Although the importance of DNA phosphodiester groups in UDG catalysis has long been recognized (*11*), and extensively studied (*4*, *6*), the catalytic potential of DNA backbone electrostatics has not been explicitly addressed experimentally for any enzyme to the best of our knowledge.

Here we apply a rigorous and novel experimental test of the energetic role of DNA phosphate groups in UDG catalysis using the tools of synthetic chemistry and free energy correlations. Our strategy was to ablate the negative charges on each of the four phosphodiester groups through the use of stereospecific methylphosphonate (MeP) substitutions. We then compared the damaging effects of these methylphosphonate substitutions on the kinetic parameters with their damaging effects on binding of a cationic 1-azadeoxyribose (1-aza-dR$^+$) oxacarbenium ion analogue to the UDG−uracil anion binary complex. This approach has allowed us to establish the relative roles of these groups in binding the neutral ground state, the transition state, and a stable chemical mimic of the ionic intermediate (*8*). The energetic effects of phosphodiester charge ablation on the activation barrier, although significant, are not found to be the omnipotent force that the computational studies suggest. Nevertheless, the results establish that Coulombic interactions with the DNA backbone are a powerful method that enzymes may employ to selectively stabilize a charged transition state over an uncharged ground state. These favorable electrostatic interactions with the substrate may account for the extraordinary stepwise mechanism for glycosidic bond cleavage catalyzed by UDG.

EXPERIMENTAL PROCEDURES

Materials. The nucleoside phosphoramidites, adenosine methylphosphoramidite, and universal support CPG[1] were purchased from Glen Research (Sterling, VA). 1-Aza-1,2-dideoxy-4α-carba-D-ribitol phosphoramidite and its methylphosphoramidite were synthesized as described previously (*12*−*14*). All the DNA substrates (see Figure 2 for abbreviations) were synthesized using standard phosphoramidite chemistry with an Applied Biosystems 390 synthesizer. The deprotection of the oligonucleotides followed normal procedures except for the methylphosphonate derivatives, in which 1,2-diaminoethane was used instead of ammonium hydroxide (*15*). All the oligonucleotides were purified by anion exchange HPLC as the first step, followed by desalting and resolving of methylphosphonate isomers using a C-18 reversed phase preparative column (Phenomenex Aqua column) and gradient elution from 0 to 30% CH_3CN in 0.1 M aqueous TEAA over the course of 3 h. AmIAA was further resolved by using an analytical reverse phase column except without TEAA (pH 9). Deoxyuridine was purchased from Sigma Chemicals and purified before each use (*4*). The purity and nucleotide composition of the DNA were assessed by analytical reversed phase HPLC and MALDI or electrospray mass spectrometry: AmApUpApA (*R* or *S*), calcd MW 1478 and found 1478; AmUpApA (*R* or *S*), ApUmApA (*R* or *S*), and ApUpAmA (*R* or *S*), calcd MW 1165 and found 1165; ApIpApA, calcd MW 1055 and found 1055; AmIpApA (*R* or *S*), ApImApA (*R* or *S*), and ApIpAmA (*R* or *S*), calcd MW 1053 and found 1053. The concentrations were determined by UV absorption measurements at 260 nm, using the pairwise extinction coefficients for the constituent nucleotides (*16*). The purification of UDG has been described previously (*17*).

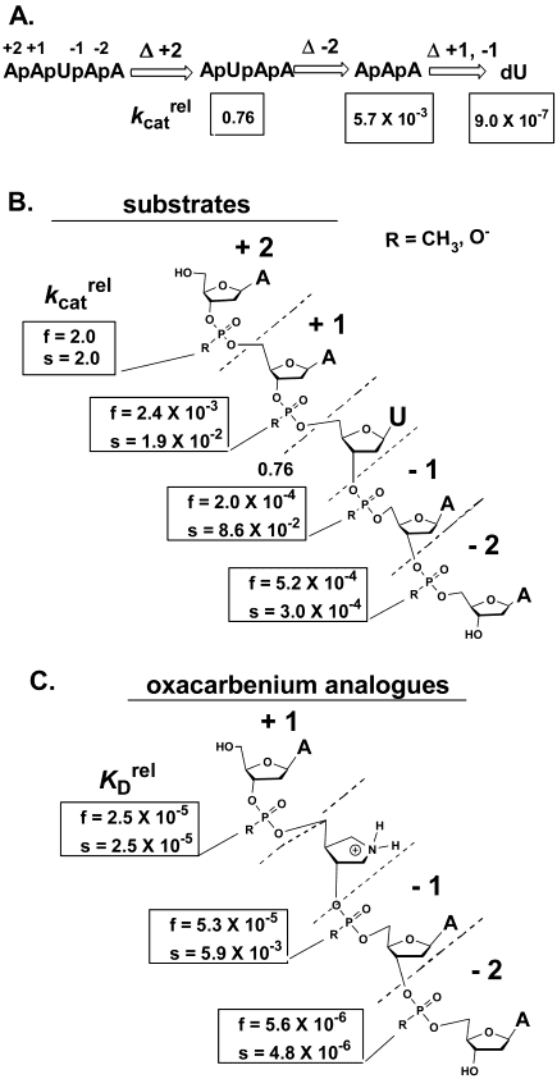

FIGURE 2: Substrates and 1-azadeoxyribose inhibitors utilized in these studies. (A) Nucleotide deletion studies ($k_{cat}^{rel} = k_{cat}^{x}/k_{cat}^{5mer}$). (B) Methylphosphonate substitution studies. The relative k_{cat} values for the fast (f) and slow (s) migrating stereoisomers are indicated (see the text). (C) 1-Azadeoxyribose oxacarbenium ion mimics. Each phosphodiester linkage was substituted with a methylphosphonate group, and the relative K_D values as compared to that of the all phosphodiester analogue were measured.

Steady State Kinetic Measurements. The steady state kinetics of uracil glycosidic bond cleavage were determined

[1] Abbreviations: TMN, buffer containing 10 mM Tris-HCl (pH 8.0), 2.5 mM $MgCl_2$, 25 mM NaCl, and 10 μg/mL BSA; MeP, methylphosphonate substituent; CPG, controlled pore glass.

at 25 °C in TMN buffer using an HPLC-based assay (*4*). Samples (20 μL) of the reaction mixtures were injected directly onto the HPLC column using a flow rate of 1 mL/min. A Phenomenex Aqua reversed phase C-18 HPLC column (250 mm × 4.60 mm, 5 μm) with the following solvent systems was used: 4mer substrates and isocratic elution with 9% CH_3CN in 0.1 M aqueous TEAA, 5mer oligonucleotide and isocratic elution with 13% CH_3CN in 0.1 M aqueous TEAA, and deoxyuridine and isocratic elution with 1.5% CH_3CN in 0.03 M aqueous TEAA. The steady state kinetic parameters k_{cat}, K_m, and k_{cat}/K_m were obtained from plots of the observed rate constants (k_{obsd}) against substrate concentration ($[S]_{tot}$) using a standard hyperbolic kinetic expression and the program Grafit 5 as previously described (*4*). As previously pointed out, the K_m values for poor substrates of UDG are equivalent to K_D values. For the best substrate used here, ApUpApA, the K_m is not identical to K_D, but the discrepancy is small because the bound substrate partitions similarly between dissociation and glycosidic bond cleavage ($k_{chem}/k_{off} = 2.8$). Thus, the k_{cat}/K_m measurements used in the free energy correlation studies are not significantly affected by this simplification. It was essential to purify the deoxyuridine substrate stock by HPLC immediately before reaction with UDG to remove trace amounts of uracil (<0.1%). For the reactions with deoxyuridine, substrate concentrations were in the range 0.2−60 mM, and the UDG concentration was 20 μM, thereby obeying the assumptions of steady state kinetics. Time courses were linear for up to 20% reaction with deoxyuridine, but because of the extremely slow rates, ≤20% turnover could be followed. Although the observation of multiple turnovers was not possible, the extremely slow rate of the chemical step, and the weak rapid equilibrium binding of deoxyuridine and the products, virtually require that the measurements provide steady state kinetic parameters. For the MeP-containing substrates, the substrate and UDG concentrations were in the range of 0.2−3.2 mM and 0.2 μM, respectively, and more than 20 enzyme turnovers were followed. Control experiments were performed to show that in the absence of UDG no detectable uracil was formed over the same time period with each substrate.

Dissociation Constants for 1-Azadeoxyribose (I)-Containing DNA. The dissociation constants for binding of the 1-azadeoxyribose analogues (Figure 2C) to the UDG−uracil anion complex were determined as previously described using competition binding measurements in which a 2-aminopurine (2-AP)-labeled 19mer duplex abasic analogue DNA (ϕ) was displaced from the enzyme−uracil complex (*8*). The binding parameters were obtained by computer simulation using the program Dynafit (*18*).

RESULTS

Defining the Minimal Active Substrate for UDG. Four substrates of UDG were initially prepared, each successively shortened to remove one of the nucleotides proposed to be essential for activity (Figure 2A and Table 1). We have previously established that a 5mer single-stranded oligonucleotide, $A^{+2}pA^{+1}pU^{-1}pA^{-2}pA$, allows UDG to achieve its full catalytic potential, with a single-turnover cleavage rate that is essentially identical to that of a duplex 19mer substrate (~110 s^{-1}) (*8*, *17*). Although k_{cat} for the best UDG substrates is partially limited by product release, these small single-stranded substrates have sufficiently fast product off-rates that k_{cat} is similar to the single-turnover rate (*8*). Thus, we use the k_{cat} value for this 5mer substrate as a reference to assess the relative damaging effects of removing nucleotide groups or making MeP substitutions (i.e., $k_{cat}^{rel} = k_{cat}^{x}/k_{cat}^{5mer}$; see Figure 2A and Table 1). Removal of the +2 nucleotide from ApApUpApA to form ApUpApA produced only a small change in k_{cat} ($k_{cat}^{rel} = 0.76$), but successive removal of the +1, −1, and −2 nucleotides resulted in decrements in rate as large as 9.0×10^{-7} (Figure 2A). A surprising result from this initial analysis was that UDG accepted a simple deoxyuridine nucleoside as a substrate. This minimal substrate, which has no anionic groups at all, has a k_{cat} for hydrolysis one million-fold lower than that of the reference substrate. Although this is a large number, it makes it unlikely that phosphodiester electrostatics could lower the activation barrier by more than 8.3 kcal/mol.[2] This value defines an upper limit for the electrostatic contributions to catalysis because it includes effects from deleting other substrate groups that promote catalysis. For instance, previous work has identified many cooperative interactions involving the DNA bases, deoxyribose, and the phosphodiester backbone (*4*, *6*).

Table 1: Nucleotide Deletion Effects on the Steady State Kinetic Parameters of UDG[a]

substrate	k_{cat} (s^{-1})	K_m (μM)	k_{cat}/K_m (μM^{-1} s^{-1})
ApApUpApA	21 ± 2	0.5 ± 0.1	42 ± 9
ApUpApA	16 ± 0.3	1.0 ± 0.1	15 ± 1.4
ApUpA	0.12 ± 0.01	$(4.3 \pm 0.5) \times 10^3$	$(2.8 \pm 0.4) \times 10^{-5}$
U	$(1.9 \pm 0.2) \times 10^{-5}$	$(6.0 \pm 1.3) \times 10^3$	$(3.2 \pm 0.8) \times 10^{-8}$

[a] Kinetic parameters were determined at 25 °C in TMN buffer.

A Framework for Interpretation of Methylphosphonate (MeP) Substitution Effects. Although methyl substituents are roughly isosteric with oxygen, it would be naive to interpret the energetic effects of MeP substitution as arising solely from the annihilation of charge on the nonbridging phosphodiester oxygens. Thus, a methyl substitution effect is most conservatively interpreted as an upper limit for the electrostatic contribution to the kinetic or binding parameter under consideration. Our emphasis on using k_{cat} measurements for these comparisons has the advantage of canceling out energetic perturbations that are common in both the ground state and the transition state. This is true because $-RT \ln k_{cat}^{rel}$ measures the change in the activation barrier free energy due to the MeP substitution (*19*). Thus, the increase in the activation barrier upon MeP substitution for a nonbridging oxygen provides an estimate of the favorable interaction

[2] For this statement to be true, the transition state structure must not change significantly when the phosphodiester groups are removed. If upon removal of these groups the lowest-energy saddle point on the free energy reaction surface corresponds to a more associative transition state (an anti-Hammond effect) (*1*), then the electrostatic contribution could be larger than 9.2 kcal/mol. Although this interesting issue remains to be thoroughly investigated, a large change in transition state structure would appear unlikely because individual removal of the two enzyme groups that electrostatically stabilize the transition state (His187 and Asp64) did not change the family of KIEs as compared to those of the wild-type enzyme (R. M. Werner and J. T. Stivers, unpublished observations). In addition, the uncatalyzed reaction appears to be fairly dissociative as judged by the β_{lg} of −1 (*2*). Whether an intermediate can still exist in the UDG active site after the removal of multiple phosphodiester groups that stabilize the transition state by as much as 8 kcal/mol is currently under investigation.

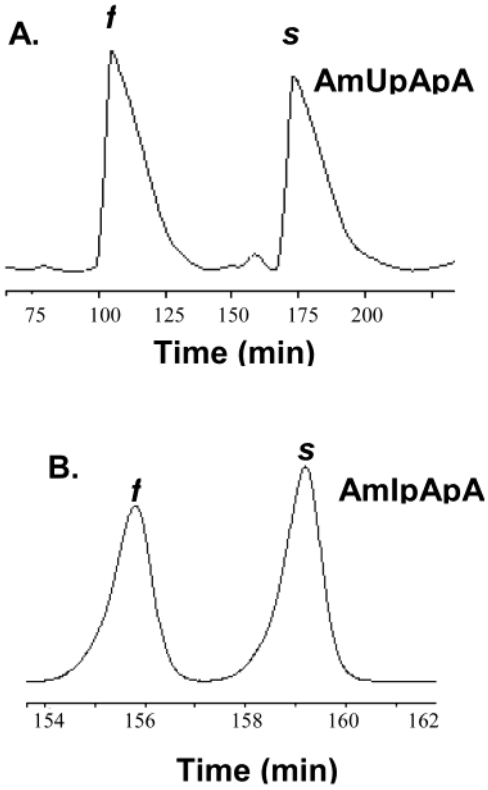

FIGURE 3: Resolution of the fast (f) and slow (s) migrating methylphosphonate stereoisomers of AmUpApA and AmIpApA using reverse phase HPLC (see Experimental Procedures). Abbreviations: m, methylphosphonate; p, phosphodiester; I, 1-azadeoxyribose.

energy of the anionic oxygen with the cationic transition state as compared to the neutral ground state. Nevertheless, the above approach could still tend to overestimate electrostatic effects because methyl substitution could also introduce larger steric conflicts in the transition state than in the ground state. In this work, we test this possibility by comparing the MeP effects with those obtained from nucleotide or phosphodiester deletion at the same position. A final estimate for the electrostatic contribution to transition state stabilization is provided by comparing the effect of MeP substitution on binding of the neutral substrate with that for binding of the cationic 1-aza-dR$^+$ oxacarbenium ion analogue (Figure 2C).

The +2 Phosphodiester Is Not Important in Catalysis or in Determining the Transition State Structure. The above nucleotide deletion studies indicated that interactions with the +2 nucleotide were not important in lowering the activation barrier. We then tested whether stereospecific substitution of uncharged MeP groups for the nonbridging oxygens at the +2 phosphodiester had a significant effect. As shown in Figure 3A, the MeP stereoisomers can be cleanly resolved by HPLC. We did not stereospecifically assign these stereoisomers, and merely refer to them as "f " and "s" to distinguish the fast and slow migrating isomers, respectively, during elution from the HPLC column. This ambiguity in assigning the stereochemistry has no impact on any conclusions in this study.

QM/MM studies suggested that the negative charge contributed from the +2 phosphodiester lowered the activation barrier by 5 kcal/mol (*10*). In contrast, we found no effect upon MeP substitution at this position. Thus, by two

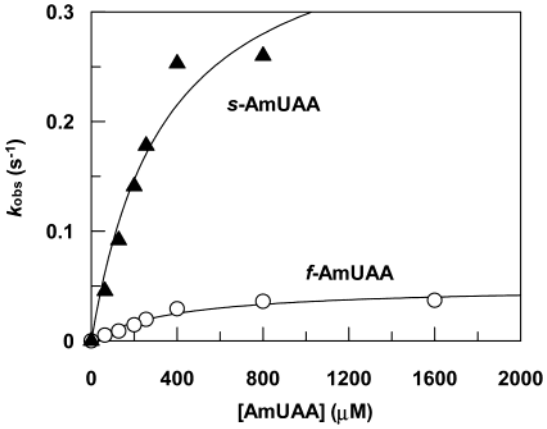

FIGURE 4: Steady state kinetic measurements for cleavage of the glycosidic bond of deoxyuridine in the +1 methylphosphonate-substituted 4mers. Data for the fast and slow migrating stereoisomers are shown. The curves are nonlinear regression fits to a standard hyperbolic kinetic expression. The complete kinetic results are reported in Tables 1 and 2.

separate measures, complete removal of the A^{+2}p and substitution of the +2 oxygens with methyl groups, the interactions at this position are found to have no effect on the activation barrier. Importantly, the A^{+2}p does not contribute to the dissociative transition state structure, because the previous kinetic isotope effect studies were performed using the pUAG trimer that lacks a +2 nucleotide (*20*). In addition, the +2 (and +1) phosphodiester groups are not essential for productive binding, because the crystal structure of UDG bound to the hydrolysis products of the UAAp trinucleotide is indistinguishable from the structure of UDG with 10mer duplex DNA (*6*, *21*). In conclusion, we can find no substantive catalytic interaction of UDG with the +2 phosphodiester.

Importance of the +1, −1, and −2 Phosphodiesters. After establishing that the 4mer substrate possessed all of the required substrate functionalities to promote full activity, we systematically introduced stereospecific MeP substitutions at the +1, −1, and −2 positions (Figure 2B). Representative kinetic data for MeP substitution at the +1 position are shown in Figure 4. These substitutions lead to large deleterious effects [k_{cat}^{rel}(f) = 2.4 × 10^{-3}, k_{cat}^{rel}(s) = 1.9 × 10^{-2}], suggesting that charge ablation and/or steric effects are significantly damaging at this position. The measured effects, corresponding to 3.6 and 2.4 kcal/mol of destabilization, respectively, are likely to be dominated by charge ablation and not steric effects because previous studies have measured a similar effect upon removal of a +1 hydroxypropyl phosphodiester linkage (Sp) from the SpUpApA oligonucleotide to generate UpApA ($\Delta\Delta G$ = 2.7 kcal/mol) (*4*). These compatible measurements, in combination with the similar findings from the 1-aza-dR$^+$ binding studies below, provide an estimate of 2.4−3.6 kcal/mol for the electrostatic contribution from this phosphodiester group.

The two MeP stereoisomers at the −1 position produce very different damaging effects on k_{cat} [k_{cat}^{rel}(f) = 2.0 × 10^{-4}, k_{cat}^{rel}(s) = 0.086]. Since a pure electrostatic effect should be largely independent of the MeP stereochemistry (because either stereoisomer effectively removes the charge), then the much larger damaging effect for the f isomer corresponding to 5.1 kcal/mol must result from other causes such as steric conflicts. The possibility that the difference between the fast

and slow isomers might be due to differing orientations of the two phosphodiester oxygens relative to the charged sugar is unlikely, as both oxygens are pointed away from the anomeric center with very similar O−C1′ distances (4.5 and 4.8 Å) (Figure 1). Supporting this interpretation, the smaller damaging effect of the s isomer, corresponding to an increase in the activation barrier of 1.5 kcal/mol, is similar to the 3.1 kcal/mol detrimental effect of deleting a hydroxypropyl phosphodiester (pS) from the −1 position of SpUpS ($k_{cat}^{rel} = 0.0048$) to generate SpU ($k_{cat}^{rel} = 2.9 \times 10^{-5}$) (*4*). Thus, the best experimental estimate of the electrostatic stabilization provided by the −1 position is in the range of 1.5−3.1 kcal/mol.

There is excellent agreement between the large damaging effects of the two MeP substitutions at the −2 position [$k_{cat}^{rel}(f) = 5.2 \times 10^{-4}$, $k_{cat}^{rel}(s) = 3.0 \times 10^{-4}$]. These effects are 10−20-fold larger than the effect arising from complete removal of the −2 pA group ($k_{cat}^{rel} = 5.7 \times 10^{-3}$) (Figure 2A). We have previously proposed a large role for the −2 phosphodiester as a handle for assembling the active site in a productive conformation (*4*). Because of the highly cooperative nature of the interactions at this position, the observed effects are likely to include many other contributions other than electrostatics, which are not easily extracted from the data. Nevertheless, the results provide an upper limit estimate for electrostatic contributions from the −2 position in the range of 3−4.9 kcal/mol.

Are Electrostatic Interactions with the Phosphodiester Groups Used To Stabilize Developing Charge in the Transition State? We recently discovered that DNA containing a cationic 1-aza-dR$^+$ group (Figure 2C) was a tight binding inhibitor of UDG that bound specifically to the enzyme−uracil anion product complex, suggesting that this inhibitor was acting as a stable chemical mimic of the oxacarbenium ion intermediate (K_D = 100−500 pM) (*8*, *9*). Here we investigate the effects of MeP substitution on the binding affinity of 1-aza-dR$^+$-containing DNA to the UDG−uracil anion complex. Our working hypothesis is as follows: if removal of the phosphodiester anions destabilizes the developing positive charge on the sugar in the transition state, then the same energetic destabilization should be observed for binding of the 1-aza-dR$^+$-containing DNA. We resolved the two MeP stereoisomers at each position of the 1-aza-dR$^+$ DNA using HPLC (Figure 3B), and then measured the binding affinity of the all phosphodiester 4mer, and each MeP-substituted analogue to the UDG−uracil anion complex using a competitive displacement fluorescence assay (Figure 5) (*8*). The all phosphodiester 4mer (ApIpApA, where I is 1-aza-dR$^+$) binds to the binary complex with a K_D of 530 pM (Figure 5A), which is indistinguishable from the previously measured affinity of an 11mer DNA strand containing the same 1-aza-dR$^+$ group (*8*). Substitution of MeP groups at the +1, −1, and −2 positions resulted in very large 5.9 × 10^{-3} to 4.8 × 10^{-6}-fold effects on the binding affinity (Figure 2C and Table 3). Representative binding data for the −1 MeP-substituted 4mers are shown in panels B and C of Figure 5.

To test the hypothesis that the phosphodiester anions interact similarly with the dissociative transition state and the cationic inhibitor, we plotted log K_D for the series of MeP-substituted inhibitors against log k_{cat}/K_m for the corresponding substrates (Figure 6). This linear correlation has a

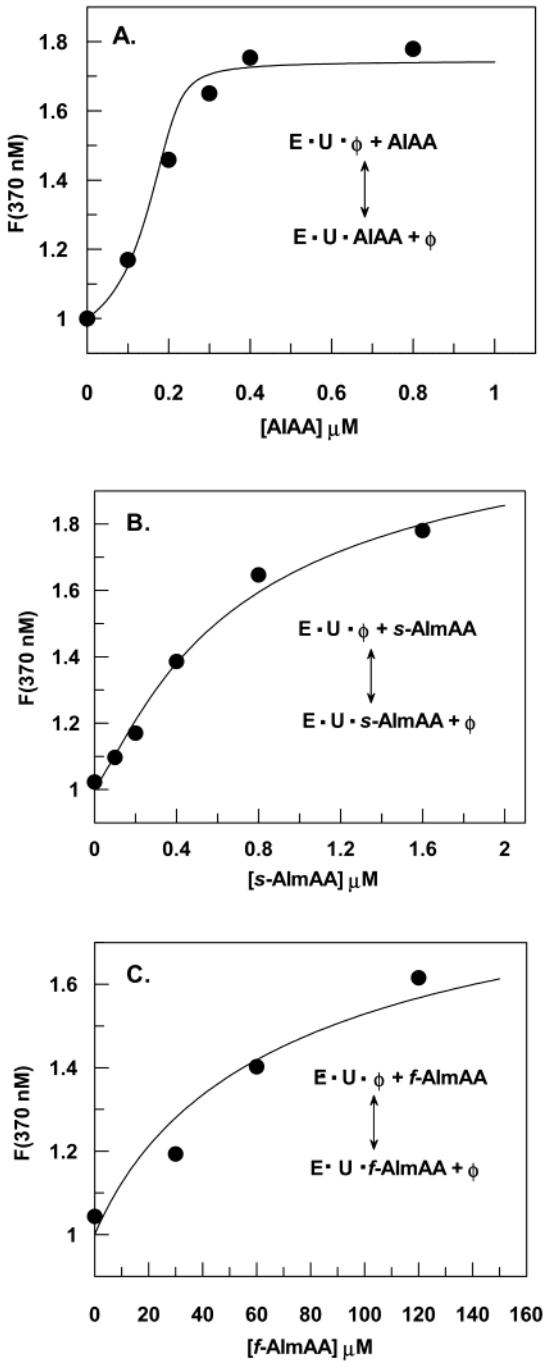

FIGURE 5: Measurements of the extent of binding of 1-azadeoxyribose analogues to the UDG−uracil anion complex at pH 8.0 by displacement of the fluorescent abasic DNA (ϕ). The increase in 2-aminopurine fluorescence at 370 nm is plotted. (A) Binding of the all phosphodiester 4mer. (B) Binding of the −1 methylphosphonate-substituted 4mer (slow isomer). (C) Binding of the −1 methylphosphonate-substituted 4mer (fast isomer). The curves were obtained by nonlinear regression fitting of the data using the program Dynafit (*18*). The dissociation constants are reported in Table 3.

slope β of −1 ± 0.1, indicating that the transition state resembles the inhibitor, and that each of the phosphodiester groups of the DNA has a similar favorable interaction with the transition state and the cationic inhibitor (*22*, *23*). A plot of log K_D against log K_m also shows a linear correlation, but the slope is only 0.5 ± 0.03 (Figure 6). Thus, the phosphodiester groups are also used for ground state stabilization of the substrate, but the interactions are weaker than in the

Table 2: Effects of Methylphosphonate Substitution on the Steady State Kinetic Parameters of UDG[a]

substrate	k_{cat} (s^{-1})	K_m (μM)	k_{cat}/K_m (μM^{-1} s^{-1})
f-AmApUpApA	43 ± 3	6.8 ± 1.2	6.4 ± 1.2
s-AmApUpApA	42 ± 2	2.8 ± 0.5	15 ± 2
f-AmUpApA	$(5.0 \pm 0.5) \times 10^{-2}$	402 ± 98	$(7.5 \pm 1.7) \times 10^{-5}$
s-AmUpApA	0.40 ± 0.06	345 ± 116	$(7.0 \pm 1.4) \times 10^{-4}$
f-ApUmApA	$(4.3 \pm 0.4) \times 10^{-3}$	175 ± 38	$(1.3 \pm 0.3) \times 10^{-5}$
s-ApUmApA	1.8 ± 0.1	20 ± 3	$(9.2 \pm 1.5) \times 10^{-2}$
f-ApUpAmA	$(1.1 \pm 0.1) \times 10^{-2}$	531 ± 148	$(2.1 \pm 0.4) \times 10^{-5}$
s-ApUpAmA	$(6.4 \pm 0.5) \times 10^{-3}$	342 ± 68	$(2.3 \pm 0.5) \times 10^{-5}$

[a] Kinetic parameters were determined at 25 °C in TMN buffer. Abbreviations: m, methylphosphonate; p, phosphodiester.

Table 3: Effects of Methylphosphonate on Binding of 1-Aza-dR^+ to the UDG−Uracil Anion Complex[a]

inhibitor	K_D (μM)	inhibitor	K_D (μM)
ApIpApA	$(5.3 \pm 3.0) \times 10^{-4}$	s-ApImApA	0.09 ± 0.04
f-AmIpApA	21 ± 10	f-ApIpAmA	95 ± 30
s-AmIpApA	21 ± 10	s-ApIpAmA	110 ± 46
f-ApImApA	10 ± 7		

[a] Abbreviations: I, 1-azadeoxyribose residue; m, methylphosphonate; p, phosphodiester.

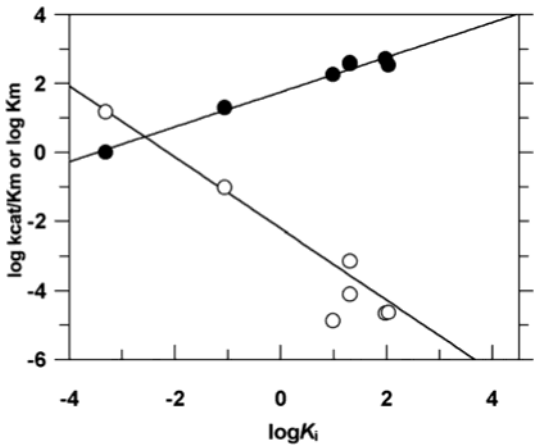

FIGURE 6: Linear free energy correlations for binding of the MeP-substituted 1-azadeoxyribose analogues and deoxyuridine substrates. The empty circles show the correlation between log k_{cat}/K_m for the MeP-substituted substrates and log K_D for the corresponding MeP-substituted 1-azadeoxyribose analogues. The slope of the line is -1 ± 0.1. The filled circles show the correlation between log K_m for the MeP-substituted substrates and log K_D for the corresponding MeP-substituted 1-azadeoxyribose analogues. The slope of this line is 0.5 ± 0.03.

transition state, consistent with the development of favorable electrostatic interactions as the charged transition state is approached.

DISCUSSION

Energetic Limits for Substrate Autocatalysis. The removal of the anionic charge of the DNA backbone through methylphosphonate substitution is a useful and reasonably nonperturbing approach to addressing the role of phosphodiester electrostatics in enzyme catalysis. Introducing methylphosphonates at the +1, −1, and −2 positions of the UDG substrate produces substantial effects on binding the neutral ground state (K_m effects), and even greater destabilizing effects in the ionic transition state (k_{cat}/K_m effects) (Table 2). This implies that direct interactions with the phosphodiester groups are used to stabilize the ground state in which the deoxyuridine sugar is neutral, and that long-range electrostatic interactions from these groups provide additional stabilization of the developing charge on the sugar in the transition state. This conclusion is strongly supported by the two free energy correlations shown in Figure 6. MeP substitution at each position produces the same incremental change in binding free energy for the cationic oxacarbenium ion analogue and the substrate in its transition state conformation ($\beta = -1.0$), yet substitution has a much weaker effect on binding of the neutral ground state ($\beta = 0.5$). These results provide further support for the contention that 1-aza-dR^+ is acting as a transition state mimic for the UDG reaction (*8*, *9*).

We can estimate the electrostatic contributions for lowering the activation barrier described by k_{cat} from the range of energetic effects arising from MeP substitution and phosphodiester deletion. These energy estimates fall in the range of 6.3−11.5 kcal/mol as judged by simple summation of the individual effects at the +2, +1, −1, and −2 positions. This energy range may be compared with the 8.3 kcal/mol activation barrier that was measured for the minimal substrate dU that lacks all phosphodiester groups (Table 1). The high-end estimate of 11.5 kcal/mol is undoubtedly biased upward because the −2 phosphodiester is involved in an intricate network of cooperative interactions that prevents accurate estimation of the electrostatic contribution from this group alone (*4*, *6*). Thus, the values in the range of 6.3−8.3 kcal/mol appear to provide the most reasonable estimates of the contribution from phosphodiester electrostatics. We do not believe that summation of these energetic effects is entirely justified, but this analysis allows us to compare the measured effects with those that have been computed using QM/MM approaches (*10*).

Comparing Computation and Experiment. The previous QM/MM study led to the conclusion that electrostatic effects arising from the +2, +1, −1, and −2 phosphodiesters contributed 17.5−21.9 kcal/mol toward lowering the activation barrier of the glycosylase reaction catalyzed by human UDG (*10*). These energetic values were obtained by calculating the height of the activation barrier defined by k_{cat} in the presence and absence of charges on the phosphodiester groups. These computed values exceed the experimental estimates by 9.2−15.6 kcal/mol, and even exceed the entire catalytic power of *Escherichia coli* UDG (16 kcal/mol) (*4*). An alternative explanation that the catalytic power of human UDG is significantly greater than that of the *E. coli* enzyme is negated because we have measured nearly identical rate constants for both enzymes using the 4mer substrate AUPA, where P is the fluorescent nucleotide 2-aminopurine. For human UDG, $k_{cat} = 15 \pm 2.5$ s^{-1}, $K_m = 10 \pm 3$ μM, and $k_{cat}/K_m = 1.5 \pm 0.4$ μM^{-1} s^{-1}, which may be compared with the previously published values for the *E. coli* enzyme (*2*): $k_{cat} = 13.5 \pm 0.9$ s^{-1}, $K_m = 4.7 \pm 0.9$ μM, and $k_{cat}/K_m = 2.9 \pm 0.6$ μM^{-1} s^{-1}.

Although our experiments can only measure the net energetic effects of these phosphodiester substitutions or deletions, and could therefore easily overestimate the pure electrostatic contribution of these phosphodiester groups, it is difficult to reconcile a large computed electrostatic effect when experimental ablation of the charged group produces little damaging effect. There are two interactions of UDG

with its substrate that were indicated to be very important on the basis of computation, yet experiments have been shown to be inconsequential. The first interaction involves the +2 phosphodiester, which was calculated to contribute 5 kcal/mol, yet our experiments show it is unimportant for lowering the activation barrier (Figure 2A,B). The second interaction involves His148 of human UDG (His67 in *E. coli*). This side chain is observed to bridge the +2 phosphodiester and the attacking water molecule, and was calculated to be doubly protonated ($pK_a = 9.2$). Computations indicated that the positive charge on His148 destabilized the transition state by 6.0−8.2 kcal/mol. However, Krokan and colleagues have constructed the H148L mutant enzyme and found that the DNA binding and catalytic activity of the mutant was decreased by less than 50% from that of the wild-type enzyme (*24*). Moreover, the pH dependence of k_{cat} for the *E. coli* enzyme is independent of pH in the range of 7−10.5 (*17*). Both of these experimental observations are inconsistent with the proposed anticatalytic role of His148.

A likely source for the deviation between experiment and computation is the computational estimation of the effective dielectric constant for the enzyme active site. There is currently no experimental method for measuring the effective dielectric constant in the UDG active site. However, if the dielectric constant were extremely low, it would be expected that removal of the catalytic Asp64 might lead to much tighter binding of the anionic DNA substrate because of a decrease in electrostatic repulsion between the negatively charged aspartate and the phosphodiester groups of the substrate (Figure 1). In fact, the D64N mutant does bind DNA more tightly than the wild-type enzyme, but the effect is worth less than 1.8 kcal/mol (*9*, *25*). It is hard to imagine that the stabilizing effects of the phosphodiester groups on the cationic transition state could be much greater than this value, given the even greater distance between the phosphodiesters and the anomeric carbon atom, and the $1/r$ dependence of the electrostatic interaction (Figure 1). This observation suggests that the effective dielectric in the immediate vicinity of the anomeric carbon is not as low as the computational models indicate.[3]

A more general question is whether computational zeroing of the charges in a static structural model and then summing the individual energetic effects can provide a fundamental understanding of enzymatic catalysis. Even if it is assumed that computational approaches for handling solvent shielding and dielectric are adequate for modeling a highly charged enzyme active site like that found for UDG, this approach cannot illuminate the additive, cooperative, and anti-cooperative energetic interactions between substrate and enzyme functional groups that give rise to catalysis and specificity. Such complex binding interactions have been shown to be individually quite modest for UDG (*4*, *6*), but collectively amass to its rate enhancement of 10^{12}-fold (16 kcal/mol). Thus, it seems improbable that enzymatic catalysis can be deeply understood by the simple summation of computed energetic effects any more than experimentalists have been able to explain catalysis by summation of mutagenesis effects. The attribution of these effects to additive electrostatic contributions misses some of the most fascinating and important aspects of the mechanism of this master catalyst.

DNA Backbone Electrostatics: General Implications for Enzymatic Catalysis. Despite the computational overestimation of the electrostatic contributions provided by the phosphodiester groups, the original substrate autocatalysis proposal is qualitatively substantiated by these experimental measurements (*8*). It is attractive to suggest that the unusual mechanism of UDG, which likely involves a discrete oxacarbenium ion intermediate, is facilitated by the additional favorable electrostatic environment provided by the anionic DNA backbone. The only other enzyme that has been suggested to follow a similar stepwise mechanism is the RNA glycohydrolase, ricin A chain (*26*). It is intriguing that other nucleoside hydrolases follow exploded S_N2 mechanisms that involve more bond formation to the nucleophile and less bond cleavage to the leaving group. Thus, these two glycohydrolases that act on DNA and RNA substrates take advantage of a catalytic tool that is provided by the substrate, and which contributes to the unprecedented transition state structures and discrete intermediates. The generality of this mechanism awaits determination of the transition state structures for other DNA and RNA glycohydrolases.

[3] Other explanations for the differences between the computational and experimental results involving differential solvation of the free phosphodiester and MeP substrates would not seem likely because the energetic comparisons described here reflect the free energy barrier between the bound substrate and the transition state (i.e., k_{cat} effects). Thus, possible differences in solvation of the free analogues are not involved in these measurements. In addition, differences in solvation between the various bound substrates are not likely to be a significant source for the discrepancies between computation and experiment, because similar estimates of the energetic contribution of the phosphodiester groups are obtained by MeP substitution and phosphodiester deletion. These significantly different substrates would be expected to be solvated differently in the enzyme active site, yet similar electrostatic effects are estimated, providing no evidence for dramatic solvation effects. It is also unlikely that a fundamental difference exists between the mechanisms and transition states for the single-stranded substrates used here, and the duplex substrate used for the computations, because (i) the reactivity of the reference 4mer single-stranded DNA is nearly identical to that of the full-length duplex DNA (*6*, *15*) and (ii) the KIE measurements were performed on a 3mer pUAG oligonucleotide (*5*).

ACKNOWLEDGMENT

We thank Lauren Morgans for the activity measurements for human UDG.

REFERENCES

1. Jencks, W. P. (1985) *Chem. Rev. 85*, 511−527.
2. Shapiro, R., and Kang, S. (1969) *Biochemistry 8*, 1806−1810.
3. Stivers, J. T., and Drohat, A. C. (2001) *Arch. Biochem. Biophys. 396*, 1−9.
4. Jiang, Y. L., and Stivers, J. T. (2001) *Biochemistry 40*, 7710−7719.
5. Parikh, S. S., Walcher, G., Jones, G. D., Slupphaug, G., Krokan, H. E., Blackburn, G. M., and Tainer, J. A. (2000) *Proc. Natl. Acad. Sci. U.S.A. 97*, 5083−5088.
6. Werner, R. M., Jiang, Y. L., Gordley, R. G., Jagadeesh, G. J., Ladner, J. E., Xiao, G., Tordova, M., Gilliland, G. L., and Stivers, J. T. (2000) *Biochemistry 39*, 12585−12594.
7. Werner, R. M., and Stivers, J. T. (2000) *Biochemistry 39*, 14054−14064.
8. Jiang, Y. L., Ichikawa, Y., and Stivers, J. T. (2002) *Biochemistry 41*, 7116−7124.
9. Jiang, Y. L., Drohat, A. C., Ichikawa, Y., and Stivers, J. T. (2002) *J. Biol. Chem. 277*, 15385−15392.
10. Dinner, A. R., Blackburn, G. M., and Karplus, M. (2001) *Nature 413*, 752−755.

11. Varshney, U., and van de Sande, J. H. (1991) *Biochemistry 30*, 4055−4061.
12. Makino, K., and Ichikawa, Y. (1998) *Tetrahedron Lett. 39*, 8245−8248.
13. Deng, L., Schaerer, O. D., and Verdine, G. L. (1997) *J. Am. Chem. Soc. 119*, 7865−7866.
14. Agrawal, S., and Goodchild, J. (1987) *Tetrahedron Lett. 28*, 3539−3542.
15. Hogrefe, R., Vaghefi, M., Reynolds, M., Young, K., and Arnold, L., Jr. (1993) *Nucleic Acids Res. 21*, 2031−2038.
16. Fasman, G. D. (1975) in *Handbook of Biochemistry and Molecular Biology: Nucleic Acids Vol. 1*, CRC Press, Boca Raton, FL.
17. Drohat, A. C., Jagadeesh, J., Ferguson, E., and Stivers, J. T. (1999) *Biochemistry 38*, 11866−11875.
18. Kuzmic, P. (1996) *Anal. Biochem. 237*, 260−273.
19. Fersht, A. (1985) in *Enzyme Structure and Mechanism*, W. H. Freeman and Co., New York.
20. Werner, R. M., and Stivers, J. T. (2000) *Biochemistry 39*, 14054−14064.
21. Parikh, S. S., Mol, C. D., Slupphaug, G., Bharati, S., Krokan, H. E., and Tainer, J. A. (1998) *EMBO J. 17*, 5214−5226.
22. Mader, M. M., and Bartlett, P. A. (1997) *Chem. Rev. 97*, 1281−1302.
23. Wolfenden, R., and Radzicka, A. (1991) *Curr. Opin. Struct. Biol.*, 780−787.
24. Mol, C. D., Arvai, A. S., Slupphaug, G., Kavli, B., Alseth, I., Krokan, H. E., and Tainer, J. A. (1995) *Cell 80*, 869−878.
25. Jiang, Y. L., Kwon, K., and Stivers, J. T. (2001) *J. Biol. Chem. 276*, 42347−42354.
26. Chen, X.-Y., Berti, P. J., and Schramm, V. L. (2000) *J. Am. Chem. Soc. 122*, 1609−1617.

BI027014X